PERFORMANCE INVESTIGATION OF SPT-20M LOW POWER HALL EFFECT THRUSTER

IEPC-2007-100

Presented at the 30th International Electric Propulsion Conference, Florence, Italy
September 17-20, 2007

A.V. Loyan*, T.A. Maksymenko †
National Aerospace University "KhAI"*, 61070 Kharkiv, Ukraine*

Abstract: The series of low power Hall Effect thrusters (LPHT) SPT-20M was developed and manufactured in STC SPE of National Aerospace University "KhAI". The main aim was to create thruster with high performances: high specific impulse and efficiency up to 40%. During SPT-20M experimental researching it was made set of tests. The LPHT magnet system was investigated with taking in account construction thermal conditions. The investigation results show that final model SPT-20M6.1 have good enough performances on power consumption less than 100 W.

Nomenclature

B	=	magnetic-field strength (Tl)
I	=	current (A)
$\dot{m}$	=	mass flow rate (mg/s)
n_e	=	electron density (m^{-3})
T_e	=	electron temperature (eV)
U	=	voltage, potential (V)
P	=	thrust (g)
N	=	power (W)
η	=	efficiency
j	=	current density (A/cm^2)
α, β	=	angle (degree)

I. Introduction

At the 70-s of XX century was approved that EP is the best decision for stationary keeping and orbit attitude. Especially Hall Effect thruster (HET) give a good account of oneself and it is developed a lot of HET models with good performances. But power consumption level of these thrusters is in 0.5-5 kW range.

On the other hand it is well known that strong tendencies of spacecraft miniaturizing and respectively installed power decreasing are occurred. The HET creating with good performances for small spacecrafts is a quite actual question and it is not decided for present time. The main developing requirement is very low power consumption – less than 100 W. Thus strong size limitations are imposed. It is seriously complicate developing of magnetic system and thruster as a whole.

In STC SPE (Scientific-Technical Centre of Spacecraft Propulsion and Energetic) of National Aerospace University "KhAI" experimental facility was constructed at the beginning of 60-s XX to study electric propulsion.

* Leading researcher, head of department, STC SPE "KhAI", loyan@d4.khai.edu
† Research assistant, STC SPE "KhAI", taras@d4.khai.edu

The work of low power Hall Effect thruster (LPHET) creating was started at 2000. The first results were published in [1]. The series of LPHT SPT-20M was developed manufactured and successfully tested. The main aim was to create thruster with high performances: high specific impulse and efficiency up to 40%.

Taking into consideration that HET efficiency and discharge chamber erosion rate are in strong dependency from magnetic field distribution we chose following directions of researching: experimentally and numerically investigate SPT-20M magnetic field distribution, magnetic system thermal behavior influence on this distribution, magnetic system optimization with the object of thrust efficiency increasing, experimental researching of efficiency raising increasing influence on a thruster lifetime.

II. Experimental Apparatus

The experimental facility consists of a stainless steel vacuum tank 1 m in diameter x 2.5 m long, prime and two turbo molecular pumps, several DC power supplies, thrust measurement system, single electrostatic probe and RPA with positioning systems, mini-spectrometer, gas supply system, digital storage oscilloscope and other measurement equipments. The vacuum tank pressure is kept a range of $7 \cdot 10^{-5}$ (on air) Torr under operations (Xe mass flow rate is up to 0.4 mg/s). A clean and high vacuum environment can be created by using the oil-free turbo molecular pump system.

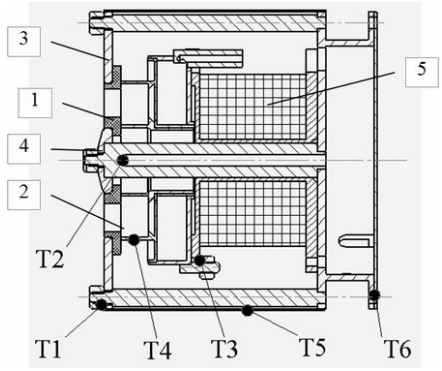

Figure 1. SPT-20M construction

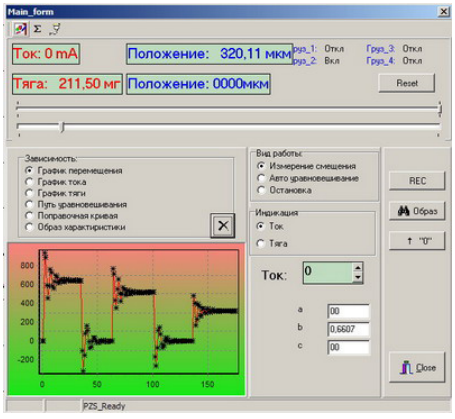

Figure 2. Calibration process (program interface)

LPHET (fig. 1) has been developed proceeding from the general conception of physical processes and existing HET schemes and also taking into consideration that is necessary to keep high value of a specific impulse and efficiency at level of power consumption 100 W and less The way of mass flow rate decreasing has been chosen from possible ways of scaling down. The radial sizes (23mm and 15mm outer and inner diameters respectively) of discharge chamber insulators (1) have been chosen from reasons of plasma density keeping equal to characteristics of known HET. It is necessary to notice, that the discharge chamber radial sizes do not allow realizing LPHET in classical configuration. Therefore the magnet core (4) construction with polar tips (3) has been developed in such a manner that the magnetization coil (5) should be placed behind the anode-gas-distributor (2). Also activity on optimization of a hollow heatless cathode-compensator was carried on [2].

Thrust balance system is of compensation type and consists of mechanical and electronic part, controlling computer interface and software. Thrust is measured by a pendulum method. Mechanical parts are 2 m long vertical bar (was made from Ti alloy), supports (made from Al_2O_3 monocrystal), liquid-metal conductor for high current and position sensor. The position of the thrust stand is detected by a CCD-sensor (non-contacting micro-displacement meter). It has high displacement sensitivity. Thrust calibration is conducted with a weight and beam arrangement which is able to apply a known force to the thrust stand under vacuum environment. We have tested the thrust balance system. Typical curve of displacement during calibration process is shown on fig. 2. With this design, friction force was small, and it resulted in no measurable hysteresis. Thermal influence is neglible small. The estimating accuracy of the thrust stand is about 3%.

The gas storage and supply system has been designed and manufactured. Gas supply system is of volume type. It includes the unit of precise and rough stabilization. Gas supply system provides such parameters:

- cathode mass flow rate 0.01-0.15 mg/sec;
- anode mass flow rate 0.1-1.2 mg/sec;
- maximum fluctuation - 1 %.

RPA system consist of RPA probe (8 mm diameter and 10 mm long without collimator and 100 mm long with it), 3-axis positioning system with position accuracy 1/200 mm and 0.5 ^{0}, controlling computer interface and

software. The RPA volt-ampere characteristics (VAC) and ion energy distribution function (IEDF) are shown on fig. 3. The accuracy of RPA VAC measurement is depends on doubling number function (typically less than several micro A, a. 0.4 %) and it show on fig. 4. The confidence coefficient is greater 0.91 when doubling number is more than 15 and we used this information on last test.

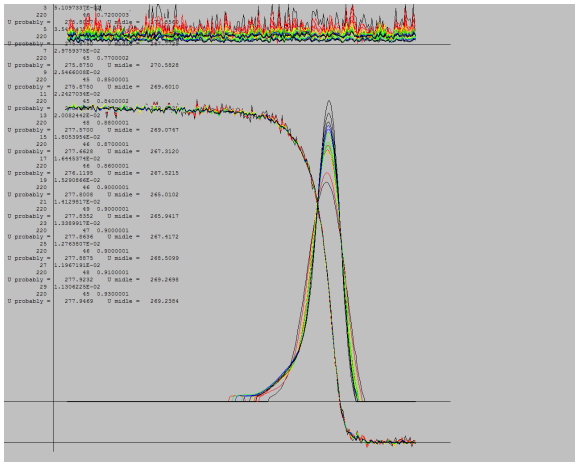

Figure 3. RPA VAC and IEED.

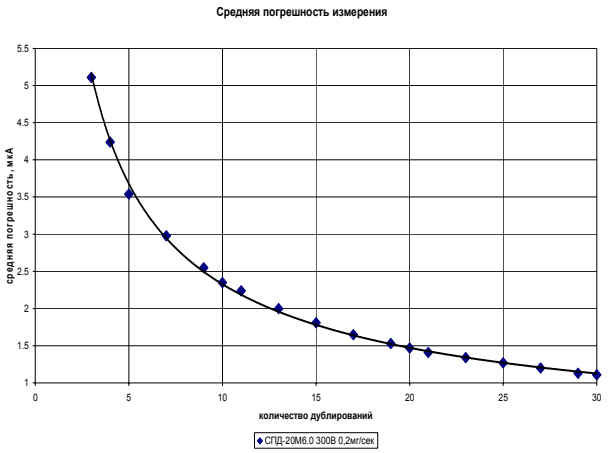

Figure 4. RPA accuracy vs. doubling number.

Single probe system consists of single probe (plate, 0.03-0.1 mm diameter), 2-axis moving system with accuracy position 1/200 mm, controlling computer interface and software. The typical VAC and EEDF is show on fig. 5, 6. Truncation error of electron temperature measurement (Te) does not exceed 15%, plasma potential – 10%, electron concentration – 40%. Accidental measurement error depends on cathode operation mode, signal noise and plasma fluctuations that could lead to large parameter variation (up to 100%). In order to improve the results validity, a statistical treatment was conducted during the measurements.

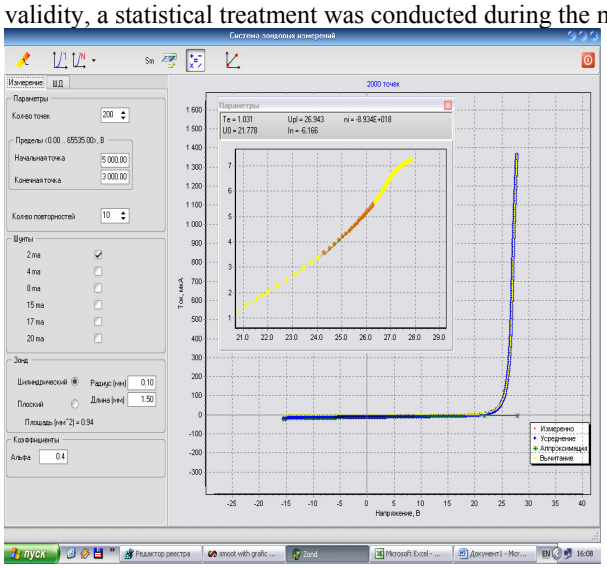

Figure 5. Single probe VAC and T_e determination.

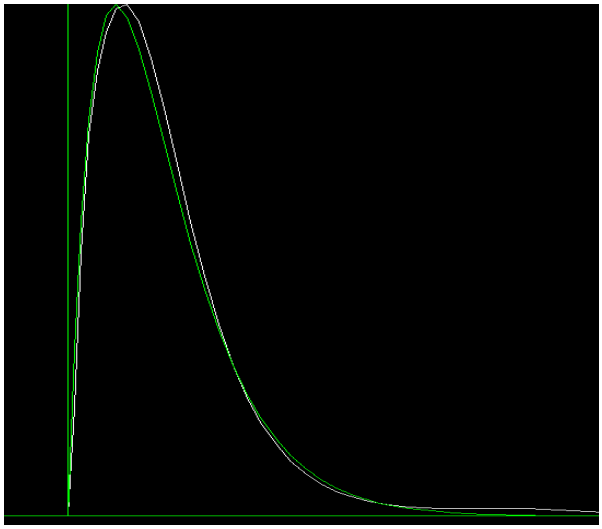

Figure 6. EEDF calculation results.

III. Research Results

Investigation of LPHET thermal behavior influence on magnetic field

We experimentally investigate magnetic field distribution inside and outside of LPHET discharge chamber. Initially main efforts were to reach a magnetic configuration similitude to classical M70 thruster type (fig. 7). This condition was not possible to execute it in view of small overall dimensions of system. However, we have reached a

magnetic field distribution which qualitatively and quantitatively demands ionization and acceleration zone formation at the expense special configuration of the anode-gasdispencer executing functions of the magnetic shield.

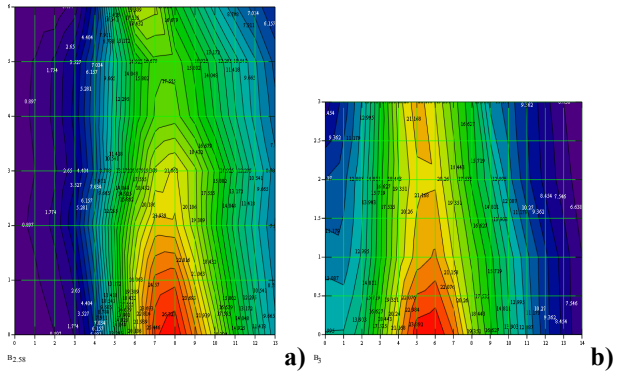

Figure 7. Tomograms of magnetic field distribution
a) M70 (Russia)
b) SPT-20M3 (Ukraine)

Further we have calculated LPHET magnetic field using final-element analysis. Initial data for creation final-element model was the information of magnetic system geometry, characteristics of the used materials, working conditions and preliminary experimental data.

Comparison shows that magnetic field modeling results have good enough agreement with experimental data as you can see on fig. 8.

During LPHET (fig. 1) tests investigation of thruster thermal behaviour has been carried out. Temperature was measured by thermocouples in following elements of the thruster: T1) external pole, T2) the central pole, T3) the anode pin, 4) the anode, 5) the protective housing, 6) the back end face of the thruster (see fig. 1). Received results are shown on fig. 9.

Limitations of experimental method not allow to receive full temperature distributions and to trace all heat-stressed sites of the thruster. We have calculated the thruster thermal behavior using final-element analysis for the solution of the given problem. The information of thruster geometry, characteristics of the used materials, working conditions and preliminary experimental data are was an initial data for creation final-element model.

The balance of heat flows was considered for the thermal task solution. It was assumed that the basic heating occurs in the coil at the expense of its resistance heating (Q_1), on walls of the discharge chamber and on the anode at the expense of a kinetic energy of the corpuscles which impacted with them (Q_2). Heat falloff occurs by radiation from a thruster surface (Q_3) and by heat conductivity through attachment elements to the interfaced construction (Q_4).

Heat flow Q_2 was determined from assumption, that part of energy of the main discharge which was not transformed into a kinetic energy of the accelerated ions and is transformed into thermal energy. Other losses bringing to efficiency decreasing are determined by ion beam defocusing and non-monochromaticity also by cathode potential drop and discharge fluctuations and expenses for ionization and radiation, etc. It is impossible to tell with large accuracy how energy losses are redistributed among themselves. Therefore the heat flow on the anode and discharge chamber walls was varied so that the sum of squares of discrepancies of the dynamic temperature characteristics received at modeling and during experiment made the minimum value for all parts of the thruster (fig. 10). As a result temperature distribution fields in the thruster (fig. 11) have been received.

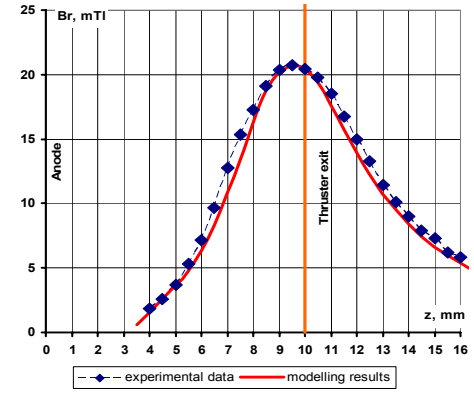

Figure 8. Radial magnetic-field strength on radially intermediate region in discharge chamber (experimental data and modeling result comparison)

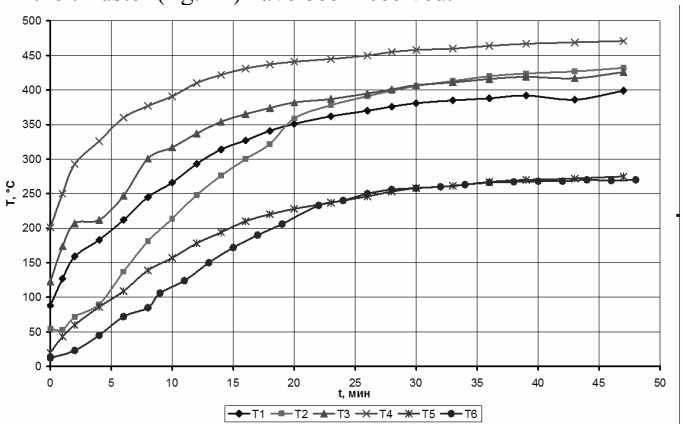

Figure 9. The LPHET temperature time history.

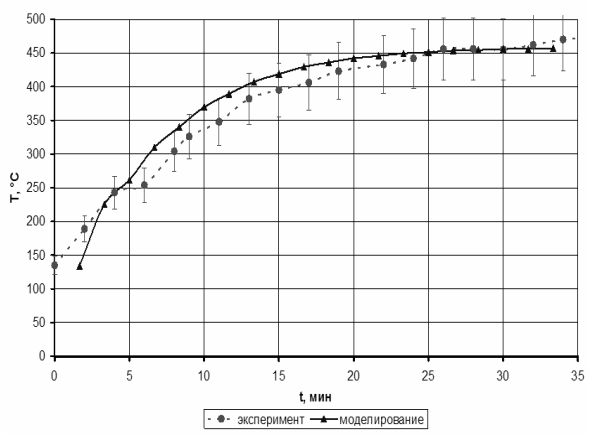

Figure 10. LPHET temperature time history (experiment and theory comparison)

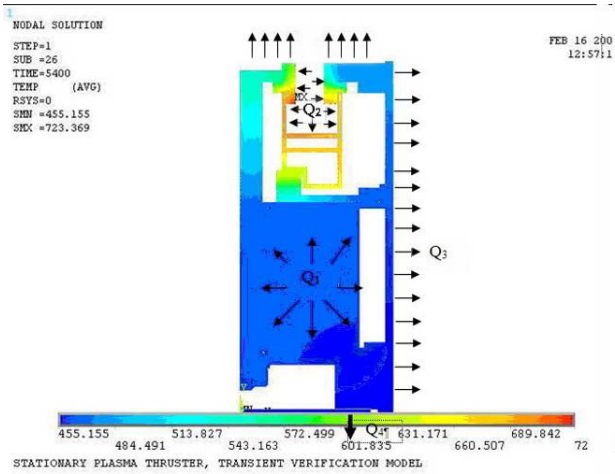

Figure 11. LPHET temperature field distribution (modeling results)

Received results show that LPHET magnetic circuit is are in a heat-stressed condition. Taking into consideration property m-materials to change the magnetic parameters it is possible to assume that magnetic field in discharge chamber will be changed (both on absolute value and force-line configuration).

We made LPHET magnetic field modeling with taking in account thermal loading and thermal dependence of material magnetic properties. Modeling results (fig. 12) show that depending on used different ferromagnetic materials for LPHET magnetic system under the presented conditions the magnetic-field strength decreasing and magnetic field distribution changing up to full destruction of a focusing configuration (for a case with a low Curie point material) are observed.

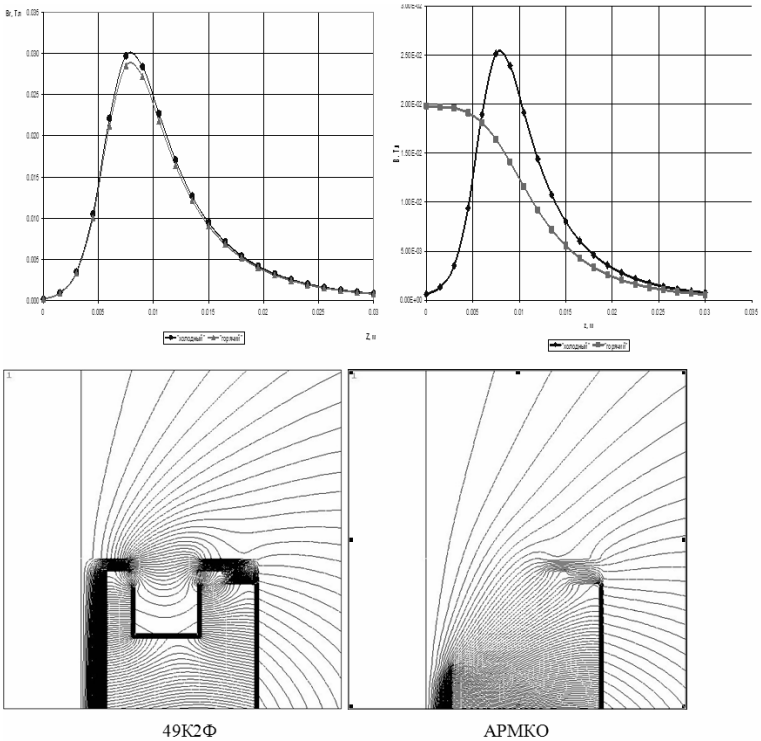

Figure 12. Magnetic field modeling results with taking in account thruster thermal behavior

It has been executed search of the rational solution for maintenance of efficiency thruster rising. We have chose G-criterion offered by Russian authors [3] for the connecting thruster efficiency with magnetic field distribution. This G-criterion characterises efficiency of electron keeping by magnetic field in ionisation zone.

The magnetic circuit geometry and heat flows on thruster construction were taking as input optimization parameters. It was necessary determine value of heat flows from experimental data. So we made series of trial LPHET at the solution intermediate stages. G-criterion was rise for each subsequent model. Thruster tests and parameters measurements were carried out on each step of optimization process and than corresponding correctives were made.

Final result shows LPHET thrust characteristics uprating (fig. 13) and efficiency increasing (fig. 14) with G-criterion rising for each next model. Thus efficiency rising on 15 % (from 23 % at the initial stage to 38 % on finishing) has been received at the 100 W power consumption.

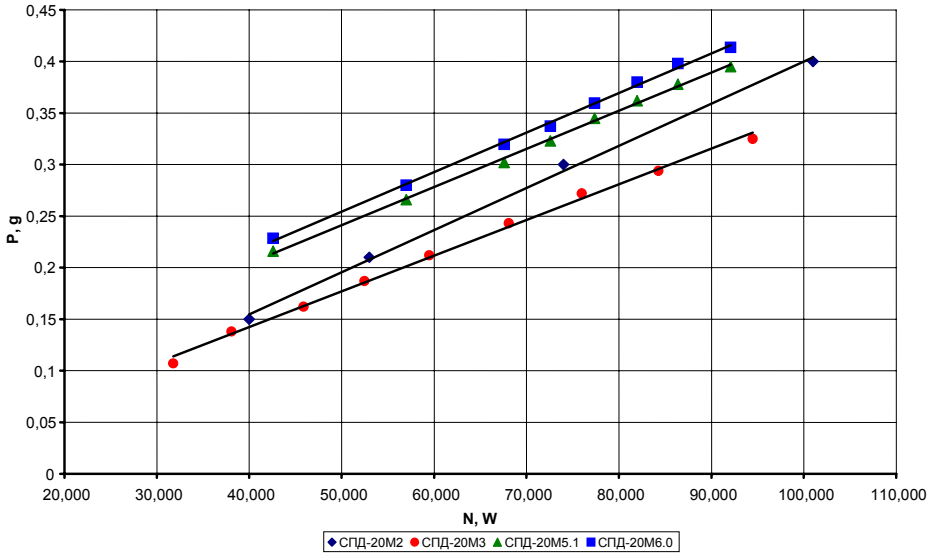

Figure 13. Thrust vs. power consumption for LPHET series.

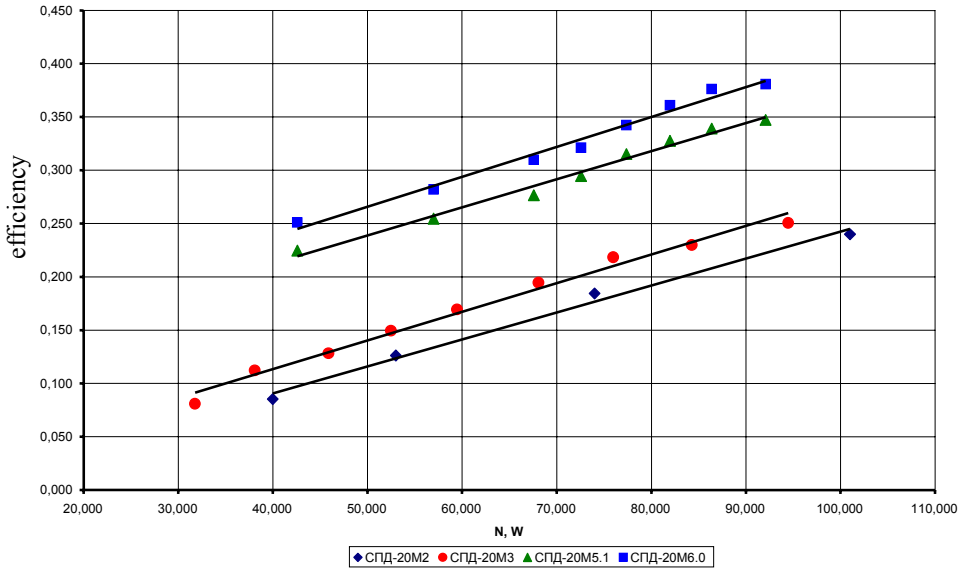

Figure 14. Thrust efficiency vs. power consumption for LPHET series.

We have made additional ion beam investigation with RPA for this phenomenon explaining. Angle divergence was calculated as "mean cosine":

$$< \cos\beta >= \frac{1}{I_i}\int_0^{\infty} 2\pi r j_{iz} \cos\beta dr ,$$

where I_i – total ion current,

r - radial distance from thruster axe,

j_{iz} - ion current density,

j_{iz} - projection on thruster axe,

$\cos\beta = \frac{j_{iz}}{j_i}$.

Also ion beam monochromatic efficiency was determined using ion energy cumulative distribution as

$$\eta_\varepsilon = \frac{\left|\int vf(v)dv\right|^2}{\int f(v)dv \int v^2 f(v)dv}.$$

It is known that ion energy increasing can bring to lifetime decreasing due to rising in total allocation of energy at the discharge chamber walls [4]. Therefore we made investigation of thruster efficiency increasing on lifetime characteristics using optical-emission method proposed by our France colleagues [5].

Ceramic type & lifetime

It is well known that discharge chamber material influence on thruster lifetime and efficiency. Therefore we made series of experiments to find new material. It is possible to increase thruster lifetime using materials with low ion sputtering coefficient. From this point of view alumina (Al2O3) much better than ABN (aluminum boron nitride) [9] but pure alumina significantly impairs thruster parameters due to secondary electron emission [6]. We have investigated set of Al2O3 ceramics with different additives. As test results show (fig. 15, 16) it is possible to keep same thruster parameters with lifetime increasing using ceramic with additive #2. Direct measurements show that speed of ceramic volume sputtering of inner ring of discharge chamber is $89 \cdot 10^{-6}$ cm^3/hour for ABN and $6.2 \cdot 10^{-6}$ cm^3/hour for alumina.

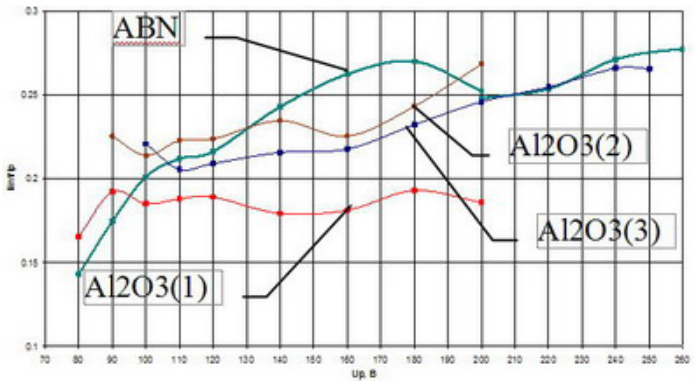

Figure 15. Discharge material influence on thruster parameters (dependence of ion current to discharge current ratio from discharge voltage)

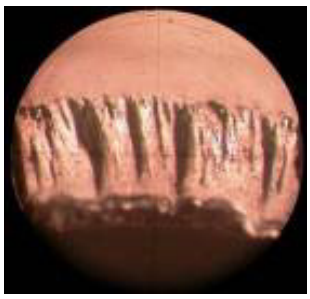
a)
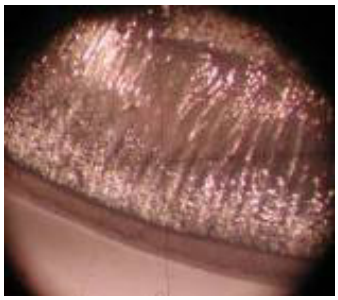
b)

Figure 16. Erosion of inside dielectric ring after 300 hours work: a – ABN, b - Al_2O_3.

Single probe and RPA measurements were made for each thruster modification. We will present only the most interesting. The map of the electron temperature, plasma concentration and plasma potential distribution near thruster tip was made by single probe system and it is show on fig. 17. Thruster axis position is on point 28 on vertical axis, 0.5mm per point for vertical axis and 1 per horizontal, T_e is in eV, $n_e * 10^{17}$ m^{-3}, U_{pl} – V. As you can see the maximum temperature, plasma density and potential are near central magnetic pole. We can not describe more detail this fact, however we connect it with specific magnet field distribution near thruster axis. Also it determines character properties micro SPT and anomaly erosion of magnet core.

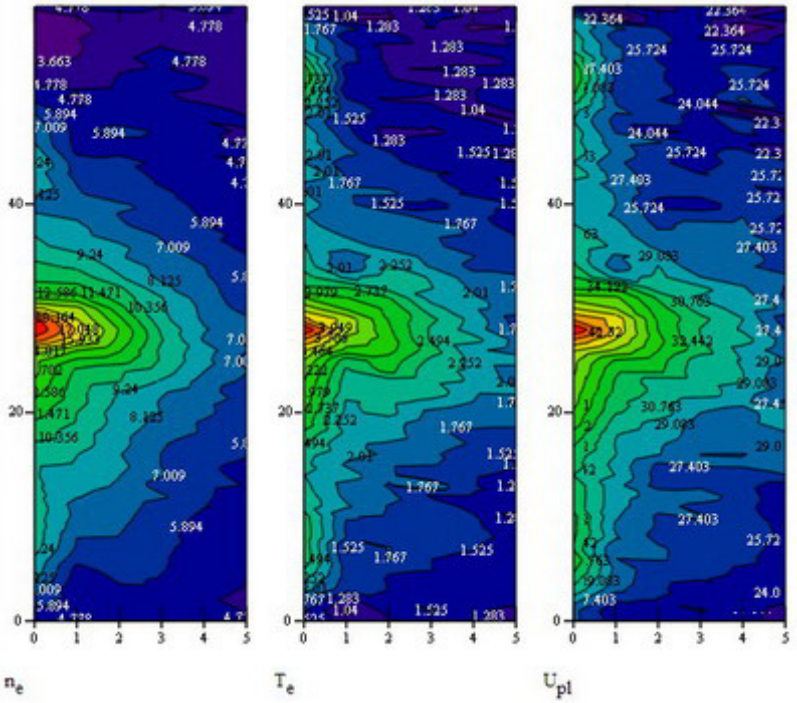

Figure 17. Single probe measurement tomograms (investigation zone 30x5mm)

Similar probe technique we used for plasma diagnostics inside thruster (special designed model SPT-M7.1 allow probe movement toward the thruster exit) along discharge channel. Fig. 18, 19, 20 show previous results.

The IEDF vs. deviation angle from thruster axis was investigated by RPA. These results are shown on fig. 21 for SPT-20M5.3 (a) and SPT-20M6.0 (b). All IEDF was normalized to one. Vertical blue line on the right correspond discharge voltage. Red line is for near thruster axis, blue – periphery. Black line on the left is ion current as function of angle divergence. The distance between IEDF line and vertical blue line is plume potential. It is 15 V for SPT-20M5.3 and 23 V for SPT-20M6.0 since thrusters was tested with different cathode modification.

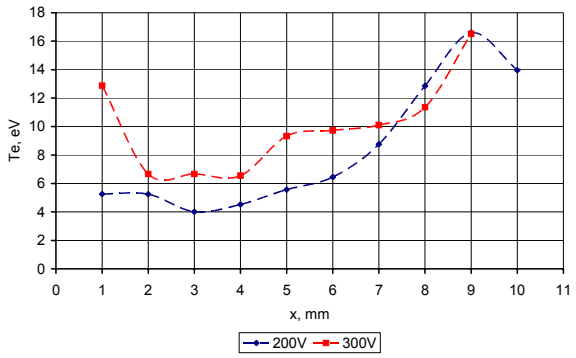

Figure 18. Electron temperature distribution along thruster discharge channel

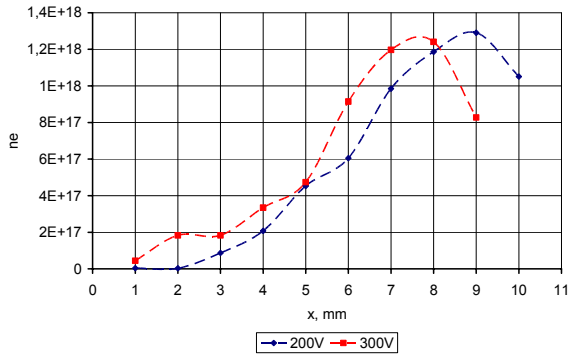

Figure 19. Electron density distribution along thruster discharge channel

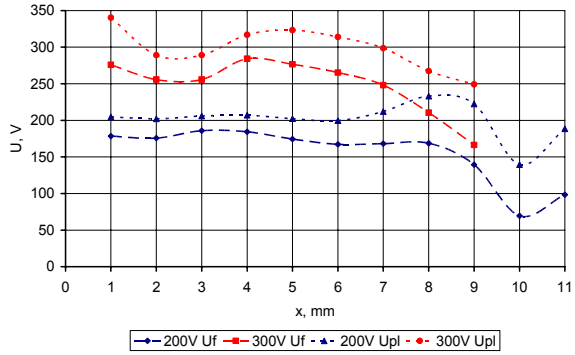

Figure 20. Floating and plasma potential distributions along thruster discharge channel

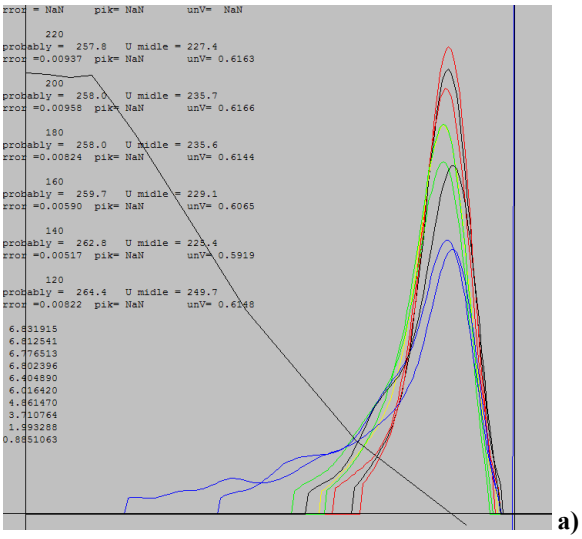

a)

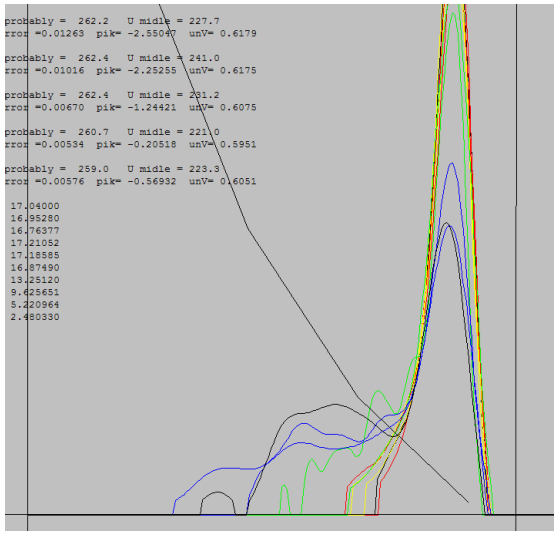

b)

Figure 21. RPA beam diagnostics test results (IEDF for (a) – SPT-20M5.3, (b) – SPT-20M6)Single probe measurement tomograms (investigation zone 30x5mm)

It is obvious that both thruster modifications has important particular. Axis zone IEDF has very well monochromatic. It displays good ion acceleration in central part of thruster. As opposed to it periphery IEDF has long tail in low energy region. It is second character micro SPT. If to compare M5.3 and M6.0 modification we can see that M6.0 IEDFs is more monochromatic. It is following on better ion focusing for older modification.

The ion divergence dependence from cathode and thruster modifications is illustrated on fig. 22. Ion divergence for M2 (green line) is great and ion current is low (bad magnetic lens). More than it is asymmetrical so mass flow rate cross anode asymmetrical to. The better modification (M3-brown line) is symmetrical and ion divergence somewhat better since magnet lens is better to. For this both experiments the distance between cathode and thruster was more than 20 thruster diameter. The cathode influence illustrate by blue line (M3 modification). The cathode location was near SPT-20 region as for flight model. This thruster has best focusing magnetic lens but asymmetrical ion current which was measured cathode cross section.

So the main intermediate conclusions after probes diagnostic are:

1. Potential distribution was measured along central line of anode. This data will be used for ion trajectory calculation.
2. Small SPT has two peculiarities: near magnet elements voltage jump and considerable non monochromatic IEDF in periphery zone of plasma flux.
3. The cathode influence can be significant.

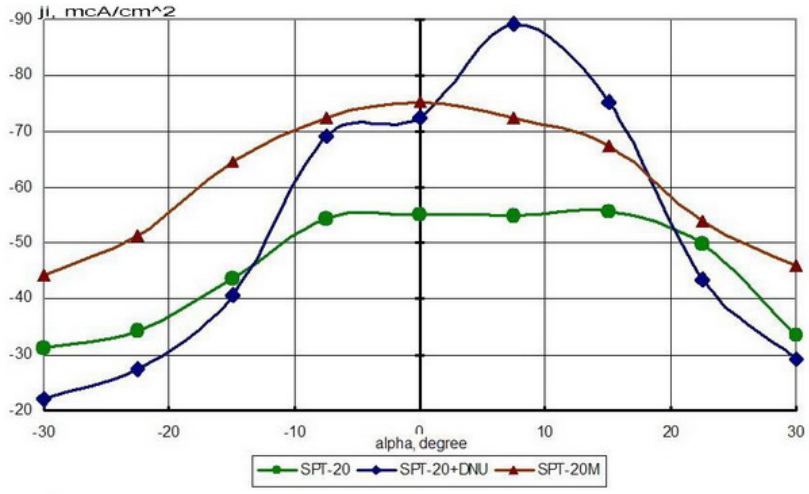

Figure 22. Plasma beam angle divergent ion.

The ion trajectory calculation was made with next admission: electric field is "trapped" in magnetic, for each force electric line exist individual potential which measure experimentally. For the first computation the electron temperature influence was take no account. Calculation scheme is show on fig. 23 (a). Left side is thruster axis, down is inside part. The color on the beginning of trajectory corresponds to maximum of ion energy after acceleration. Blue is max, red- min. On fig. 23 we display ion trajectory as function of "born-place". Another hands we modeling ionization zone location. It is immediately obvious that ion which was "born" near ionization zone has the best contribution to trust and small angle divergence (fig. 23 b, c). Three notes are important 1) ion trajectory deviation to thruster axis is larger than periphery zone; 2) ion which was "born" near external canal body is cross thruster axis; 3) ion which was "born" near internal canal body fly to periphery zone. All ions which were "born" near canal tip has small influence on thrust and angle divergence is very great (fig. 23 d, e).

So we have two important results:

1. The optimal field for acceleration zone locates inside anode nearer internal canal diameter.
2. The ions which were "born" near the thrusters tip can to produce increased erosion.

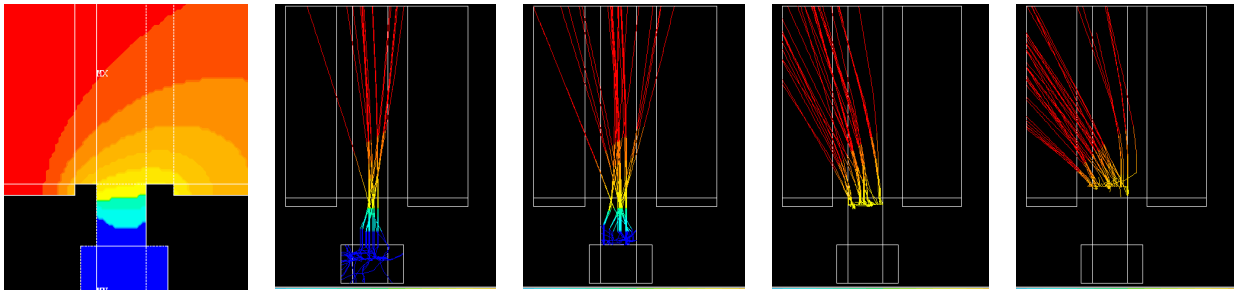

a) b) c) d) e)

Figure 23. The ion trajectory modeling results.

Neutral gas dynamic calculates by statistic methods but Monte-Carlo method was not used. More detail you can read in [7, 8].

We made full 3-d model gas flow inside the SPT discharge chamber. The software let change all geometrical dimensions include orifice diameter and angles to back side of anode, internal and external anode diameter and it length. Thruster axis is on the horizontal central line. Blue color corresponds to low neutral concentration, red – to height. One of the simulation variant is shown on fig. 24. The mass flow is calculated from the beginning of gas appearance (fig. 24 a) to stationary regime (the difference between fig. 24 c, d is small). The anode orifice locates near external corner.

The analysis show that zone with increased neutral concentration is inside discharge chamber. Moreover, the position of this zone is near non optimal for acceleration region. The optimization procedure was realized for all geometrical dimensions. The time of neutral gas delay in acceleration region was served as a criterion for optimization. The last SPT-20M6 (and higher) was manufactured with optimal gas flow geometry.

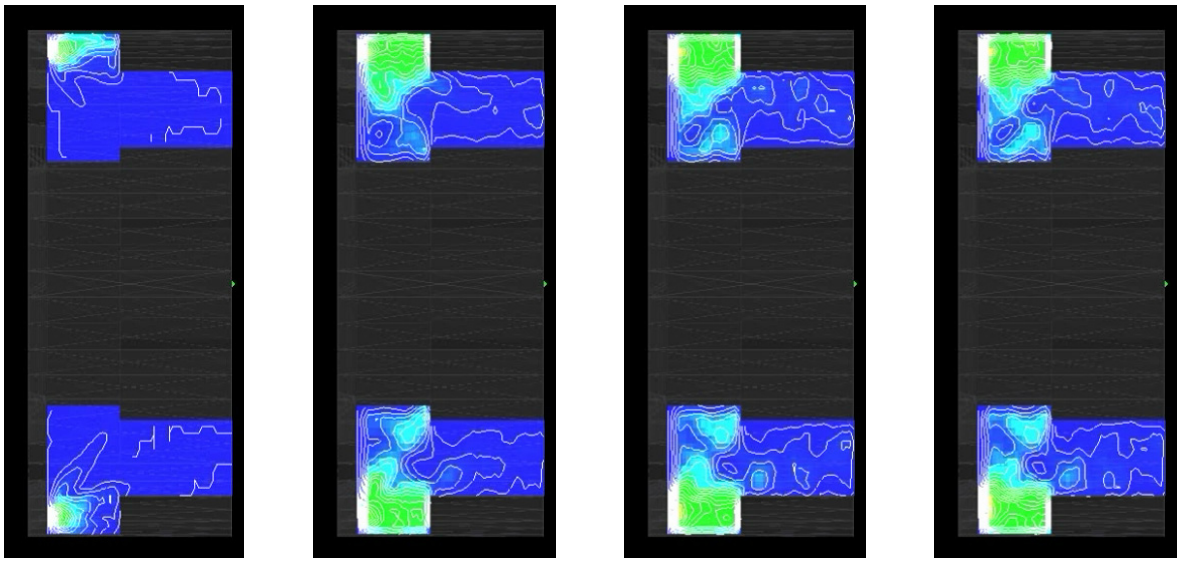

a) b) c) d)

Figure 24. Neutral gas distribution inside discharge channel history

Comparison results for 80 W power consumption level are shown at the fig. 25. G-criterion and erosion are showed as relative values for obviousness: <G>, <erosion>. It is clear to see that with G-criterion rising mean cosine, ion beam monochromatic efficiency and thrust efficiency are notably raised at the same time erosion decreasing observed. So we can say that thruster parameters improvement was achieved due to ion beam focusing, ionization and acceleration efficiency increasing as a result of magnetic field optimization taking into account thruster thermal behavior.

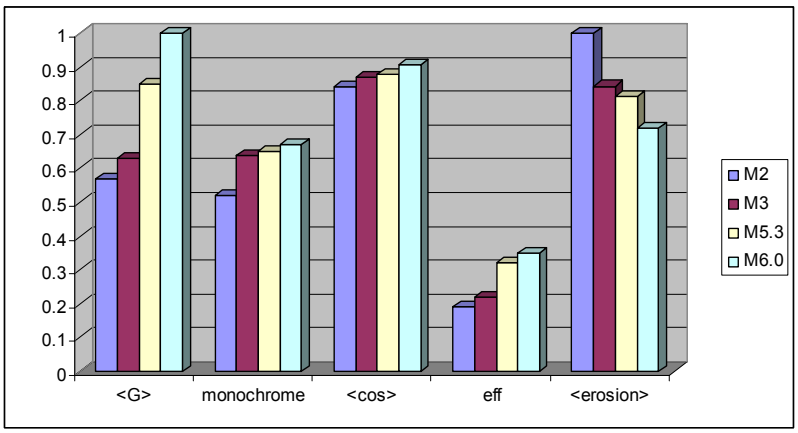

Figure 25. The LPHET series parameters comparison.

IV. Conclusion

The investigation results show that final optimized model SPT-20M6.1 have good enough performances: power consumption – less than 100 W (with magnetic coil and cathode), thrust – 4 mN, specific impulse – 1400 s, efficiency – 38%, predictable lifetime about 1000 h.

In summary we made the table 1 with main characteristics of EP system for micro and mini satellite orbit control.

The LPHET final model allows to use it onboard of different commercial mini- and micro-spacecrafts also on students' university micro-satellites and for numerous of scientific researches.

Table 1.

subsystem	manufacturing date, year	main behavior	size, mm	mass, gr.	status
SPT-20M2	2001	efficiency 22-24%	diameter 53 length 60		for scientific tests
SPT-20M3	2003	efficiency 26-29%	diameter 53 length 50	470	laboratory model
SPT-20M5.3	2005	efficiency 30-32%	diameter 42 length 50	220	engineering model
SPT-20M6.0	2006	efficiency 36-38%	diameter 42 length 45	260	qualification model
SPT-20M7	2007	efficiency up to 40%	diameter 42 length 45	200	advanced model in building
heaterless hollow cathode M1	1997	0.5A, 25-35V		120	for scientific tests
heaterless hollow cathode M3.2	2005	0.5A, 22-35V	diameter 18 length 90	43	laboratory model
heaterless hollow cathode M5.2	2006	0.25A, 18-22V	diameter 13 length 65	22	engineering model
heaterless hollow cathode M7	2007	0.25A, 16-18V	diameter 13 length 49	18	advanced model in building
PPU100M1 electric supply	2002	efficiency 55%			for scientific tests
PPU100M2.2 electric supply	2005	efficiency 85%		675	laboratory model
PPU100M3.5 electric supply	2006	efficiency 90-92%		215 without radiator	engineering model
PPU100M4 electric supply	2007	efficiency 92-94%		190 without radiator	advanced model in building
GSSS-20M3.0 gas storage and supply system	2001			1200	laboratory model
GSSS-20M3.0 gas storage and supply system	2007			370 without tank	advanced model in building
TOTAL for advanced model of EP system				**1 SPT-20, 2 cathodes 1 PPU, 1 GSSS 870**	

Acknowledgments

This research is partially supported by the STCU grant #1936 and France-Ukrainian programme Dnipro-2007. In this paper also were used materials from INTAS-03-53-3358. Authors would like to thank Koshelev N.N., A.P. Kislitsyn, Stepanushkin N.P., Pechenizkiy I.P., O.P. Rybalov and our France colleagues M. Dudeck and D. Pagnon for significant contribution and fruitful discussion.

References

1. A.V. Loyan, “Small Power SPT for Microsatellite”, Micro propulsion spatiale, Atelier CNES, 16-17 novembre 2004.

2. Nikolay Koshelev, Andriy Loyan and Oleg Rybalov “Investigation of Hollow Cathode for Low Power Hall Effect Thruster”, 30th Int. Electric Propulsion Conference, IEPC 2007-103, Florence, Italy, 16-20 Sept. 2007.

3. Experimental Investigation of Magnetic Field Topology Influence on Structure of Accelerating Layer and Performance of Hall Thruster, IEPC-2005-033.

4. Kim V., Skrylnikov A., Sidorenko E. Estimation of the power release on the SPT discharge chamber wall on base of the local plasma parameter measurements results obtained by nearwall probes // Aerospace technic and technology. - 2006. - №10(36). - P. 112-116.

5. D.Pagnon, P.Lasgorceix and M.Touzeau, “Control of the ceramic erosion by Optical Emission Spectroscopy, Results of PPS1350-G measurements”, *4th ISPC*, Cagliari, Sardinia (2004).

6. N.Gascon, M.Dudeck, S.Barral, Wall material effects in stationary plasma thruster I: Parametric studies of an SPT-100, Physics of Plasma, vol. 10, n° 10, Oct. 2003, p. 4123-4136

7. Левин С.С. Имитационное моделирование с использованием Бинарной автоматной модели //Радиоэлектронные и компьютерные системы.- 2005.- № 2. - С. 69 - 78.

8. Levin S., Loyan A., Chernyshev Yu. Event-driven modeling of three-dimensional fluid flows with use of a "hard" spheres model and finite automat model // Aerospace technic and technology. - 2006. - №8(34).-P. 179-183

9. Стационарные плазменные двигатели / Н.В. Белан, В.П. Ким, А.И. Оранский, В.Б. Тихонов: Уч. Пособие”.ХАИ, 1989.-315 с.